J Mater Sci: Mater Electron (2017) 28:16155–16164
DOI 10.1007/s10854-017-7516-z

Synthetic analysis on the IZTO thin films deposited on various plastic substrates with the buffer layer

Jong-Chan Park[1] · Yung-Sup Yoon[1]

Received: 18 May 2017 / Accepted: 10 July 2017 / Published online: 12 July 2017
© Springer Science+Business Media, LLC 2017

Abstract Buffer layers, such as SiO_2, may prevent impurities from permeating into the depositing film. Thus, the effects of buffer layer thickness on indium-zinc-tin oxide (IZTO) thin films were investigated. IZTO thin films are applied to transparent conductive oxide, and SiO_2 is used as a material for the buffer layer. Before depositing the IZTO by RF magnetron sputtering, the SiO_2 buffer layers were deposited on different plastic substrates, such as polyether sulfone, polyethylene terephthalate, and polyethylene naphthalate (PEN), by plasma enhanced chemical vapor deposition. The resulting structural, morphological, electrical, and optical properties were measured and analyzed. By using the obtained values of the electrical and optical properties, the figure of merit for transparent devices designed by Haacke was calculated. As a result, we conclude that the IZTO thin film deposited on a PEN substrate with a 30 nm thick SiO_2 buffer layer has the finest properties, which are a resistivity of 2.13×10^{-3} Ω-cm, sheet resistance of 8.875 Ω sq^{-1}, Hall mobility of 5.99 $cm^2\ V^{-1}\ s^{-1}$, carrier concentration of $3.671 \times 10^{21}\ cm^{-3}$, and transmittance of 80.26% at 550 nm. In addition, the figure of merit calculated for this sample was 12.50×10^{-3}/Ω. These results indicate that the proposed structure is suitable for flexible display devices and flexible solar cells.

✉ Yung-Sup Yoon
ysyoon@inha.ac.kr

Jong-Chan Park
parkjc0109@gmail.com

[1] Department of Electronic Engineering, Inha University, Incheon 402-751, South Korea

1 Introduction

Indium-tin oxide (ITO) is a material used in transparent conductive oxide (TCO) films and has been used widely for display devices such as liquid crystal displays (LCD), light-emitting diodes (LED), and organic light-emitting diodes (OLED), as well as in solar cells. This is because of the superior optical and electrical properties of ITO, which are due to its structural crystallization in the 300–400 °C temperature range [1, 2].

Recently, flexible display technologies have been highlighted for next generation displays. Accordingly, investigations have been carried out, by applying flexible plastics such as polyether sulfone (PES), polyethylene terephthalate (PET), polyethylene naphthalate (PEN), and polyimide (PI) to substrate materials. For example, H. Kim et al.(2001) deposited ITO on a PET substrate by using pulsed laser deposition and analyzed its resulting properties [3]. Li et al. deposited ITO on a PI substrate and analyzed its resulting properties [4]. To improve the optical and electrical properties through crystallization of ITO, the films must be deposited at high temperature or be thermally treated after deposition. Thus, the overall properties of such films deposited on plastic substrates, such as PES, PET, PEN, and PI, could be degraded because plastic tends to be deformed by heat.

Therefore, there is a necessity to make a new TCO material with excellent optical and electrical properties even at room temperature. In relation to this area of research, Teixeira et al. deposited amorphous ITO on a glass substrate by DC sputtering and analyzed its resulting properties [5]. According to their results, band gap energy was reduced by approximately 1 eV when compared with crystallized ITO and the sheet resistance was measured to be in the 230–760 Ω sq^{-1} range. Thus, the properties of such films are not good enough for them to be applied as a transparent

electrode in electrical devices. In addition, Yaglioglu et al. deposited amorphous and crystallized Indium-Zinc-Oxide (IZO) on a glass substrate by DC magnetron sputtering and analyzed the resulting properties [6]. According to their results, the electrical and optical properties of these films were better than those of amorphous ITO, but IZO has a critical drawback in that the manufacturing price of IZO targets is very high and their manufacturing process is complex.

In this research, to solve the problems mentioned, we suggest using indium-zinc-tin oxide (IZTO) instead of ITO. This compound is produced by doping zinc atoms into ITO structures. Zinc doping results in immiscibility between indium and tin atoms, thus IZTO films are formed with amorphous structures [7, 8]. Additionally, IZTO films have excellent electrical properties induced by the indium atoms contained in them, and they are more flexible compared with ITO, a rigid material. Thus, the IZTO is suitable for next-generation flexible display devices.

However, plastic has another critical drawback; it absorbs moisture and gases during the deposition process, which then permeate to the disordered parts of film being deposited as impurities [9]. Consequently, this could degrade the quality of films [10]. It has been reported that this problem can be reduced to some degree by forming a film with a high work function and low reactivity (such as SiO_2, TiO_2, HfO_2, Ga_2O_3) on substrates before depositing the TCO film. These materials may act as a buffer layer, thus prevent impurities from permeating [11, 12].

Polyether sulfone (PES) is known to be a superior plastic in regards to its optical properties, but its mechanical properties, such as tensile strength and extension strength, are poor. Polyethylene terephthalate (PET) has the lowest coefficient of thermal expansion (CTE) among plastics and is therefore an attractive option for mass production. However, its glass transition temperature (Tg), which is as important as the CTE, is also the lowest among plastics. Therefore, there is a temperature limitation. On the other hand, polyethylene naphthalate (PEN) has two condensed aromatic rings, by replacing the benzene ring in PET with naphthalene rings, as shown in Fig. 1. Due to these aromatic rings, PEN has excellent physical and chemical properties compared to PET, in addition to having the property of blocking ultraviolet (UV) rays [13, 14]. Table 1 shows a comparison between the PET (125 µm, Teijin DuPont, TETORON KEL86W) and PEN (125 µm, Teijin DuPont, TEONEX Q65HA) films in view of their main features: tensile strength, CTE, Tg, haze, and total transmittance. The naphthalene aromatic rings described above, which replace benzene rings, slightly improve PEN's tensile strength and CTE, and increase the glass transition temperature, which is a critical problem of PET films. Consequently, it might be expected that there are merits to using PEN. However, its optical properties, namely haze and transmittance, are slightly worse than those of PET, because of PEN's property of blocking UV rays. In spite of the excellent physical properties and heat-resisting property held by PEN when compared with PET, its application as substrate for display devices is unprecedented.

In this research, we utilized PES, which has superior optical properties, PET, which is the most suitable for mass production, and PEN, whose physical properties are improved by replacing the benzene rings in PET with naphthalene rings. The buffer layers, composed of SiO_2, were formed and applied before depositing the new transparent conductive oxide, IZTO. The properties of each structure were then analyzed.

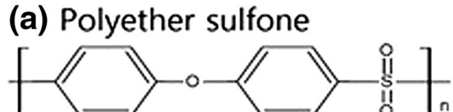

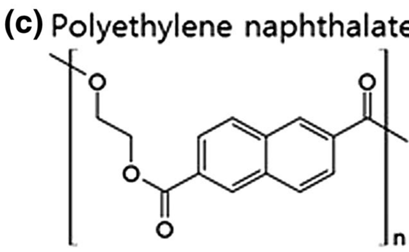

Fig. 1 Chemical structures of **a** PES, **b** PET, and **c** PEN

Table 1 Properties of PET and PEN

Property	PET	PEN
Tensile strength	232 Mpa	250 Mpa
Coefficient of thermal expansion (CTE) (150 °C, 30 min)	0.4%	0.3%
Glass transition temperature (Tg)	75 °C	120 °C
Haze	0.4%	2%
Total light transmission (TLT)	91%	87%

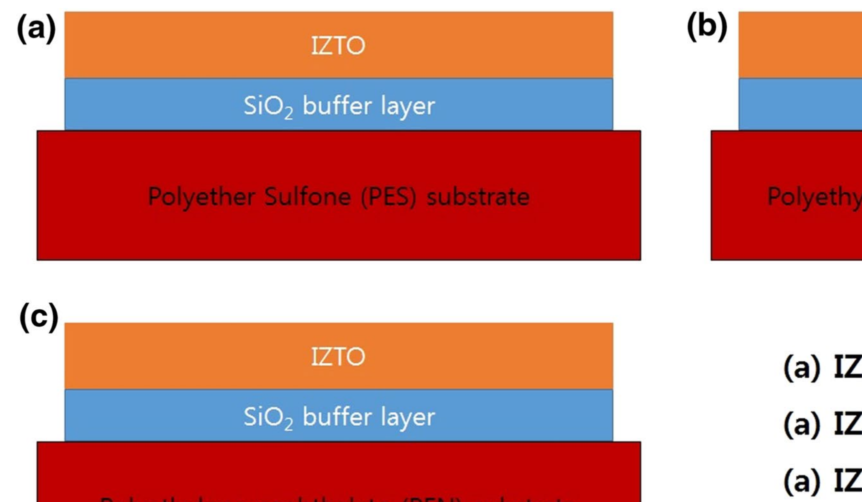

Fig. 2 Proposed structures

2 Experimental details

Experiments in this research were carried out using the structures presented in Fig. 2. Before depositing the IZTO as the TCO on PES, PET, and PEN, SiO_2 was applied as a buffer layer.

The plastic substrates, such as PES (200 nm, SUMILITE® FST-5300), PET (125 µm, Teijin DuPont, TETORON KEL86W), PEN (125 µm, teijin-dupont, TEONEX Q65HA), were cut into squares of the size of 1×1 in. Because these plastic substrates can be deformed by acetone, they were cleaned with ultrasonic cleaner in isopropyl alcohol and deionized water each for approximately 3 min. They were then dried by nitrogen gas.

Plasma-enhanced chemical vapor deposition (PECVD) was used for depositing SiO_2 as a buffer layer, with thicknesses of 10, 20, 30, 40, and 50 nm. The Table 2 shows the depositing conditions of PECVD.

A sintered 2-inch diameter IZTO (In_2O_3 90 wt%; ZnO 5 wt%; SnO_2 5 wt%) ceramic target was used in the deposition process, and the IZTO thin films were deposited by RF magnetron sputtering; the process's conditions are shown in Table 3.

Table 2 Conditions of PECVD

Working pressure	800 mTorr
Working temperature	R.T
RF power	40 W
N density	20 sccm
N_2O density	200 sccm
SiH_4 density	600 sccm

Table 3 Conditions of RF magnetron sputtering

Base pressure	4.5×10^{-6} Pa
Active gas (Ar) density	20 sccm
Working pressure	3 mTorr
Working temperature	R. T
RF power	50 W
Deposition time	10 min
Deposited thickness	160 nm

The structural and morphological properties of the deposited IZTO were analyzed using X-ray diffraction (HR-XRD, Xpert-Pro, MRD) and atomic force microscopy (AFM, SII Nano Technology, SPA400). The electrical and optical properties were analyzed using hall-effect measurements (Accent, HL5500PC) and UV–Vis spectrometry (Varian, Cary-500). Using the sheet resistance data measured by hall-effect measurements and the transmittance data for 550 nm wavelengths measured by UV–Vis spectrometry, the figure of merit designed by Haacke was calculated, which represents synthetic performance for transparent electrodes.

3 Results and discussion

Figure 3 represent the X-ray diffraction patterns of the IZTO thin films with 0–50 nm SiO_2 deposited on several plastic substrates. In the case of PES substrates (Fig. 3a), these films only have halo patterns at 32°, thus we can conclude that these films have an amorphous structure. In

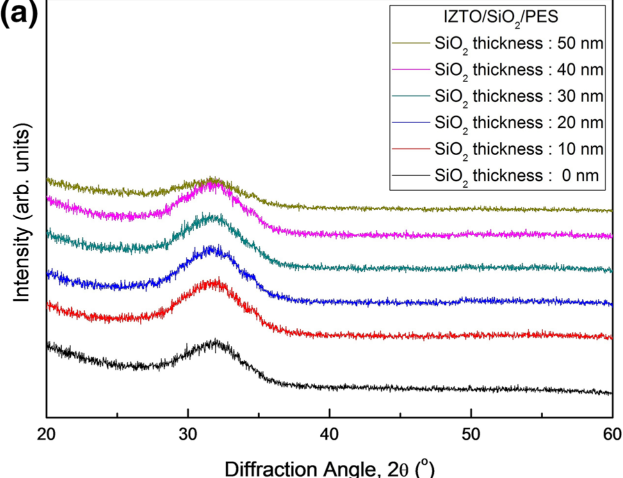

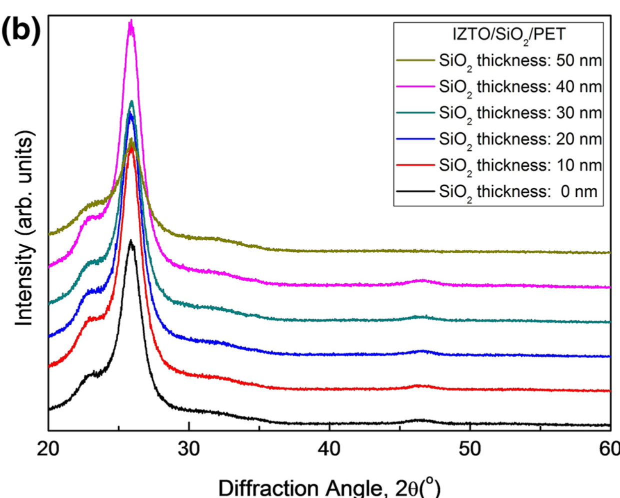

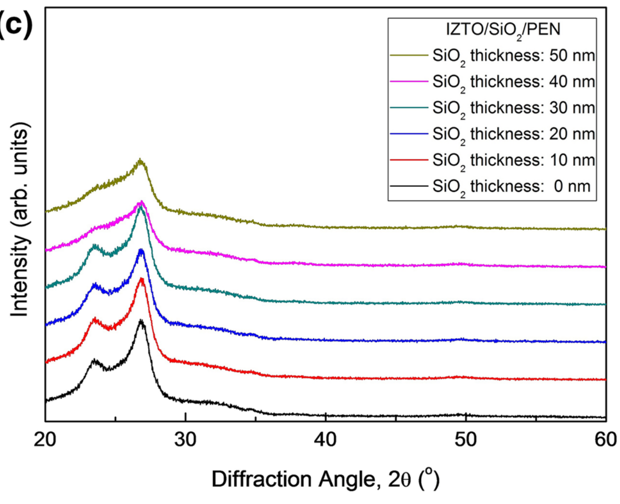

Fig. 3 X-ray diffraction patterns of IZTO films deposited on PES **a**, PET **b**, and PEN **c**

addition, the results of XRD for the IZTO films deposited on PET (Fig. 3b) and PEN (Fig. 3c) show a very extensive peak at 27° of diffraction angle 2θ, and another peak, smaller than that of 27°, at 23°. According to previous research, it has been reported that these peaks are native peaks of PET and PEN, whose structure is semi-crystalline [8, 13]. According to these facts, we can conclude that the IZTO thin films deposited on PES, PET, and PEN substrates have amorphous structures. The XRD patterns of PEN, in which the benzene rings of PET are replaced with naphthalene rings, have remarkably reduced peak intensity compared with those of PET. Thus, we can assume the semi-crystalline features of PEN were weakened, in comparison with PET's.

The AFM images of IZTO thin films deposited on PES substrates are shown in Fig. 4. For buffer layer thicknesses ranging from 10 to 50 nm, surface roughness, which is represented by the root mean square (RMS) value, was measured to be lower than 3 nm, which means the surfaces were very smooth. However, pin-holes, which extremely degrade the overall properties of the thin films, were generated. In the case of the 10 nm SiO_2 buffer layer (Fig. 4a), in particular, the film presented the most severe condition: porous film. Because the IZTO thin film is a template for the next process in device level, such as LED, OLED, LCD, and solar cells, fewer pin-holes, and cracks result in better properties. If the next process for manufacturing display device were carried out on porous IZTO thin film, that display panel would shows defects on that panel. So, we could analogize that this PES substrate is not suitable for opto-electrical device, due to the pin-holes generated on the surface of IZTO thin film deposited on PES substrates.

Figure 5 shows the AFM images of IZTO thin films deposited on PET substrates with 10–50 nm thick SiO_2 buffer layers. It seems that the IZTO thin films were successfully deposited on PET substrates without pin-holes or cracks. However, the values of surface roughness were measured to be 15.59, 16.98, 17.97, 18.11, and 17.25 nm, respectively, as the thickness of the SiO_2 buffer layer increased from 10 to 50 nm. These values are considerably worse compared with those of PES, which means that the surfaces are not smooth. This was analogized with the results obtained with X-ray diffraction shown in Fig. 3, which describe the semi-crystalline structure of PET.

The IZTO thin films deposited on PEN substrates are shown in Fig. 6. The surface roughness of IZTO thin films with no SiO_2 buffer layer were measured to be 3.576 nm, which is considerably lower than in the case of IZTO on PET. For an increasing buffer layer thickness ranging from 10 to 50 nm, the values of surface roughness were measured to be 2.772, 2.714, 2.694, 3.148, and 3.128 nm, respectively. These values are comparable with the case of IZTO deposited on PES substrates, and means that IZTO

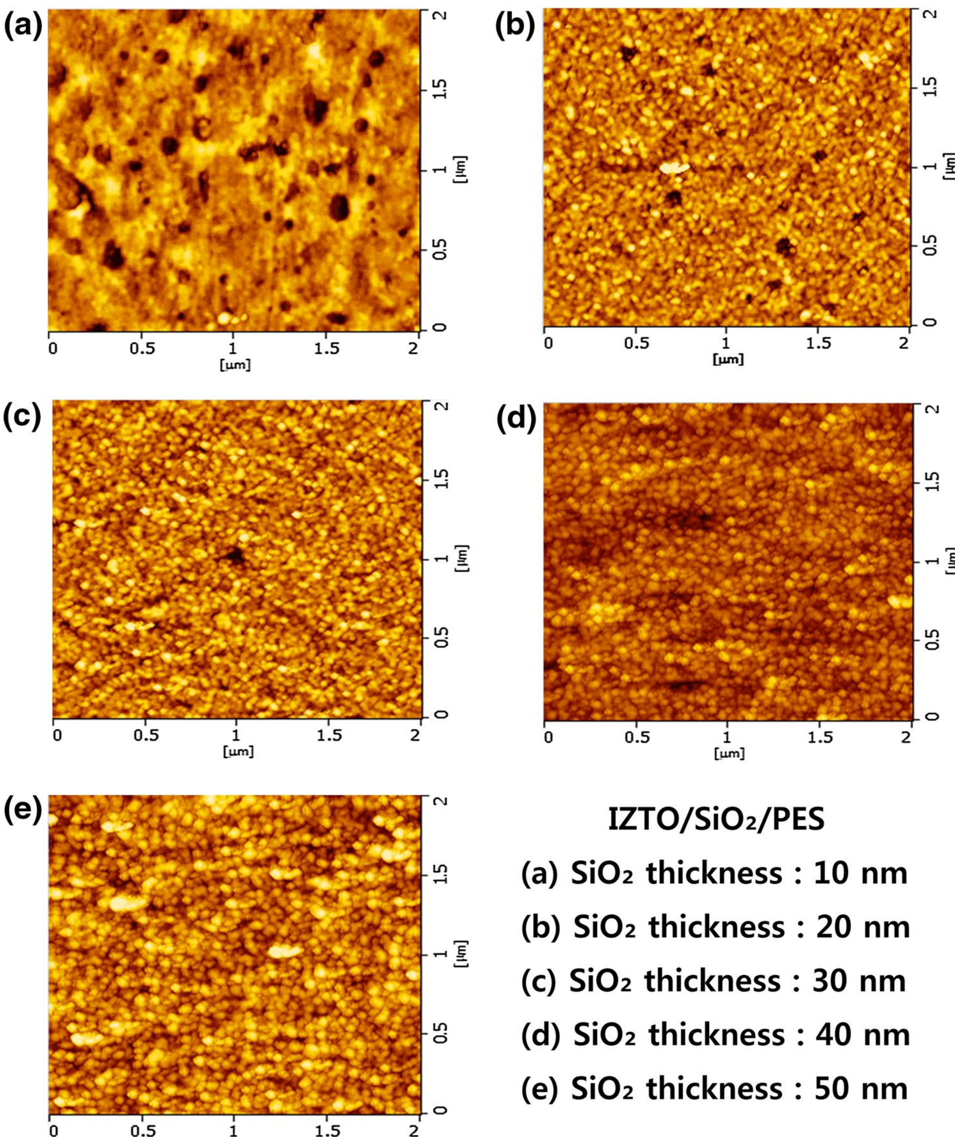

Fig. 4 AFM images (2D) of IZTO/SiO_2/PES films with different thicknesses of SiO_2 buffer layers

deposited on PEN substrate has a surface smooth enough to be applied in display devices. The buffer layer performed its role of buffer well as increasing its thickness up to 30 nm, so the surface roughness was reduced. When the thickness of the SiO_2 layer was 40 or 50 nm, however, those roughness were increased. This could be analogized by the fact that the stress induced to the substrates was relaxed and the degree of disorder increased [13].

The transmittance of the IZTO thin films deposited on (a) PES, (b) PET, and (c) PEN substrates with various thickness of SiO_2 buffer layer are represented in Fig. 7. The transmittance curves (Fig. 7a, b) of samples using PES and PET as substrates showed no remarkable differences with varying SiO_2 buffer layer thicknesses, while in the case of using PEN as a substrate (Fig. 7c), they present tangible differences compared with other cases. Consequently, we determine that the PEN substrates may be affected by the thickness of the SiO_2 buffer layer more than other substrates, and that the thickness of this SiO_2 buffer layer might be an important parameter for overall performance at the device level.

The feature of optical devices is determined by optical transmittance at wavelengths of 550 nm (T_{550}), because human's vision is most sensitive at that wavelength. Thus, the T_{550} of each film, composed of IZTO/SiO_2/PES, IZTO/SiO_2/PET, and IZTO/SiO_2/PEN were measured and are shown in Fig. 8. In the cases in which the PES and PET substrates were used, the T_{550} values are substantially identical with negligible differences as the thickness of the SiO_2 buffer layer increased. There was also a decreasing tendency. However, the samples that use PEN substrates show fluctuating T_{550} values. The highest T_{550} values measured

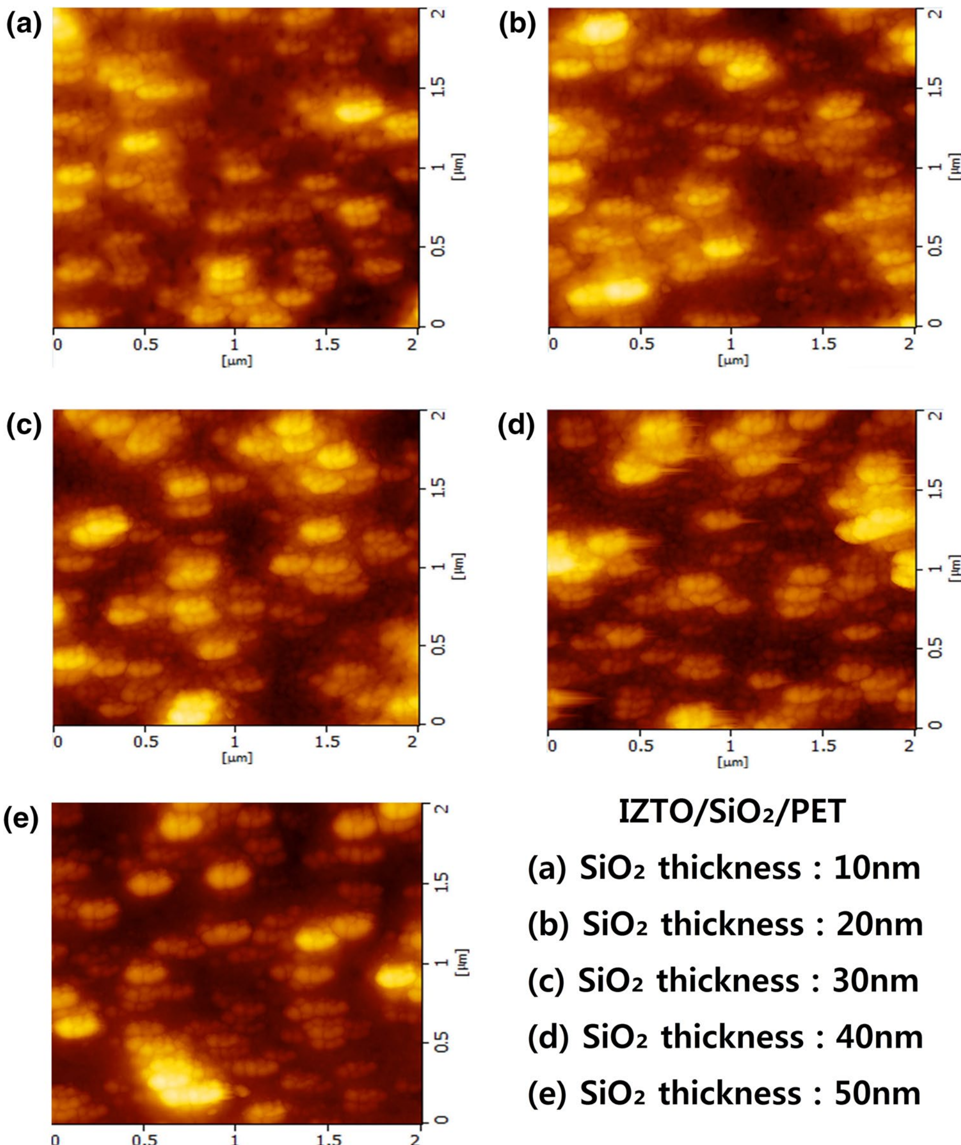

Fig. 5 AFM images (2D) of IZTO/SiO_2/PET films with different thicknesses of SiO_2 buffer layers

were 81.14% and 80.26% for buffer layer thicknesses of 20 and 30 nm, respectively. The IZTO/SiO_2/PES films have transmittance at 550 nm similar with or lower than the case of PET, and these films have pin-holes as shown in Fig. 4. We could analogize that the IZTO films deposited on PES substrates have extremely deteriorated electrical property due to the pin-holes and these films have optical property worse than the IZTO films deposited on PET or PEN. So, we concluded the IZTO thin films deposited on PES substrates are not suitable for applying to opto-electrical device and they do not need to measure the electrical property of them.

Figures 9 and 10 represent the electrical properties (resistivity, Hall mobility, and carrier concentration) of the IZTO thin films deposited on PET (Fig. 9) and PEN (Fig. 10). There are no substantial differences in the Hall mobility curves for PET substrates (Fig. 9); the Hall mobility was measured to be 5 $cm^2\ V^{-1}\ s^{-1}$, approximately. In contrast, the carrier concentration increased from $5.91 \times 10^{20}\ cm^{-3}$ to $9.03 \times 10^{20}\ cm^{-3}$ as the thickness of the buffer layer increased (≤40 nm). It has been reported that carriers in IZTO thin films are generated through substitution processes between indium and tin, and this process occurs more frequently at sharp points in the surface [13, 15, 16]. The generation of carrier in this research have the thread of connection with aforementioned report and the AFM images in Fig. 5. On this wise, increased carrier concentration minimized the resistivity to a value of 1.43×10^{-3} Ω-cm when the thickness of the SiO_2 buffer layer was 40 nm.

When the 30 nm thick SiO_2 buffer layer was formed on the PEN substrates, as shown in Fig. 10, the lowest carrier

Fig. 6 AFM images (2D) of IZTO/SiO_2/PEN films with different thicknesses of SiO_2 buffer layers

concentration value was measured to be 3.671×10^{21} cm^{-3}. The highest carrier concentration was 8.213×10^{21} cm^{-3} when using a 50 nm thick buffer layer. These results are analogous to surface roughness in Fig. 6, and this could be comprehended by the tendency explained above that carriers are generated through substitution processes and

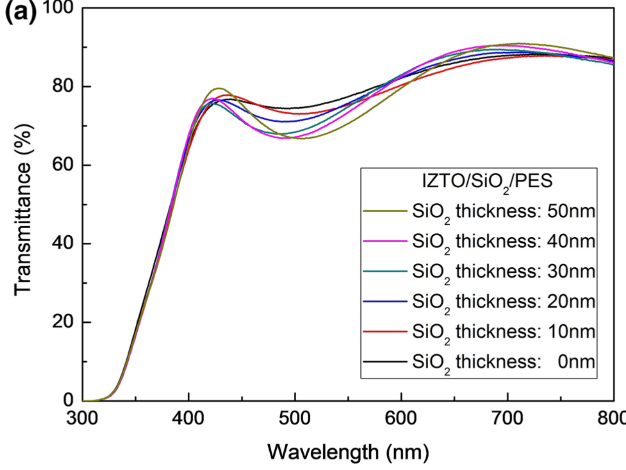

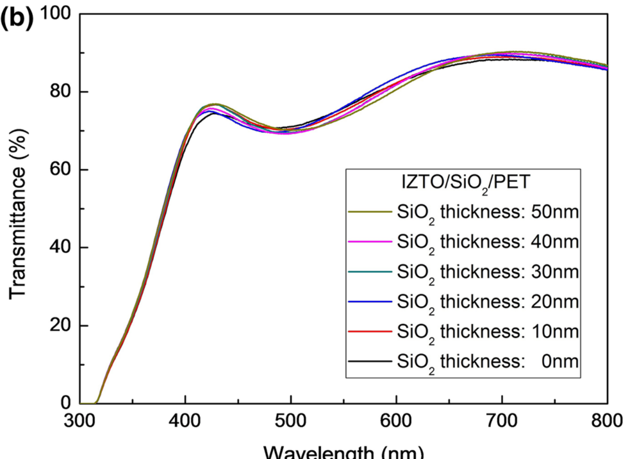

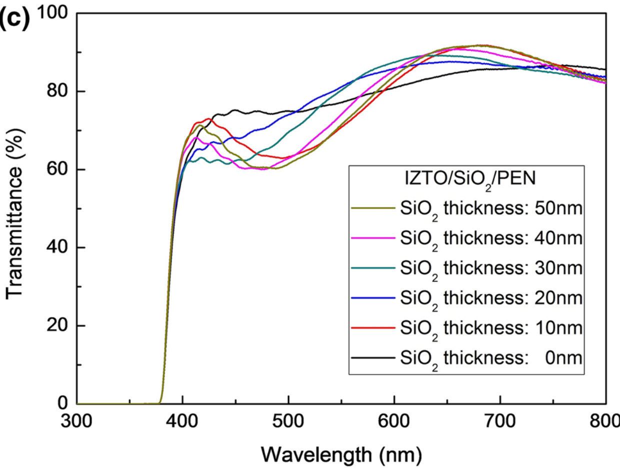

Fig. 7 Transmittance of IZTO thin films with various thicknesses of SiO_2 buffer layers deposited on **a** PES, **b** PET, and **c** PEN plastic substrates

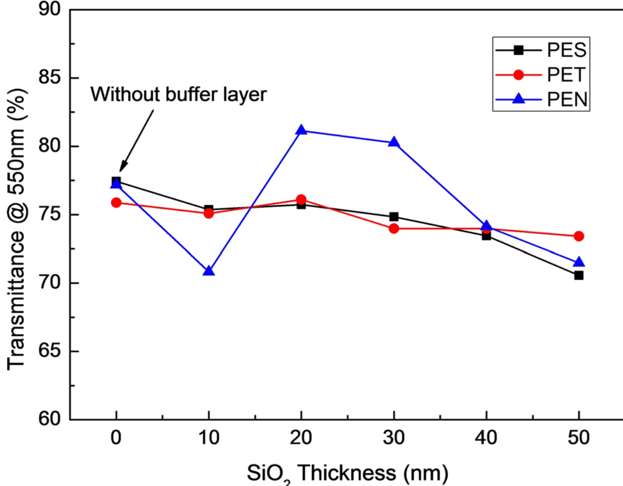

Fig. 8 Transmittance of IZTO/SiO_2/plastic substrate films for 500 nm wavelengths using PES (*black, rectangular*), PET (*red, circle*) and PEN (*blue, triangle*) substrates. (Color figure online)

this process occurs frequently at sharp points in the surface. But, all the values were high, it always exceed 10^{21} cm^{-3}. However, the largest value for Hall mobility was measured to be 5.99 $cm^2\ V^{-1}\ s^{-1}$ when using a 30 nm thick buffer layer, while the lowest value for Hall mobility was 1.37 $cm^2\ V^{-1}\ s^{-1}$ when the buffer layer was not applied. All films deposited on PEN substrates have a high carrier concentration in broad outlines, thus it seems that Hall mobility affects electrical properties more than carrier concentration because the hall mobility could affect to conductivity as much as carrier concentration [17]. According to these results, the best value for resistivity was 2.13×10^{-3} Ω-cm, when using a 30 nm thick buffer layer.

The sheet resistance (R_{sheet}) and figure of merits ($\mathbf{\Phi}_{TC}$) of the IZTO thin films deposited on PET and PEN are shown in Figs. 11 and 12, respectively. Sheet resistance was calculated by Eq. (1), using the resistivity values (**ρ**) from Figs. 9 and 10, and a film thickness t of 160 nm.

$$R_{sheet} = \frac{\rho}{t} \tag{1}$$

Additionally, the figures of merit $\mathbf{\Phi}_{TC}$ for transparent electrodes, designed by Haacke, were calculated by substituting sheet resistance obtained from Eq. (1) and T_{550} from Fig. 8 into Eq. (2) [18]:

$$\mathbf{\Phi}_{TC} = \frac{T_{550}{}^{10}}{R_{sheet}} \tag{2}$$

where T_{550} is transmittance for wavelengths of 550 nm.

The IZTO thin film deposited on PET with a 10 nm thick SiO_2 buffer layer had a sheet resistance of 121.875 Ω sq^{-1}, and then decreased to 89.375 Ω sq^{-1} as the thickness of the buffer layer increased (≤40 nm). However, the highest transmittance at 550 nm, as shown in Fig. 8, was measured to be 76.09% when using a 20 nm thick buffer

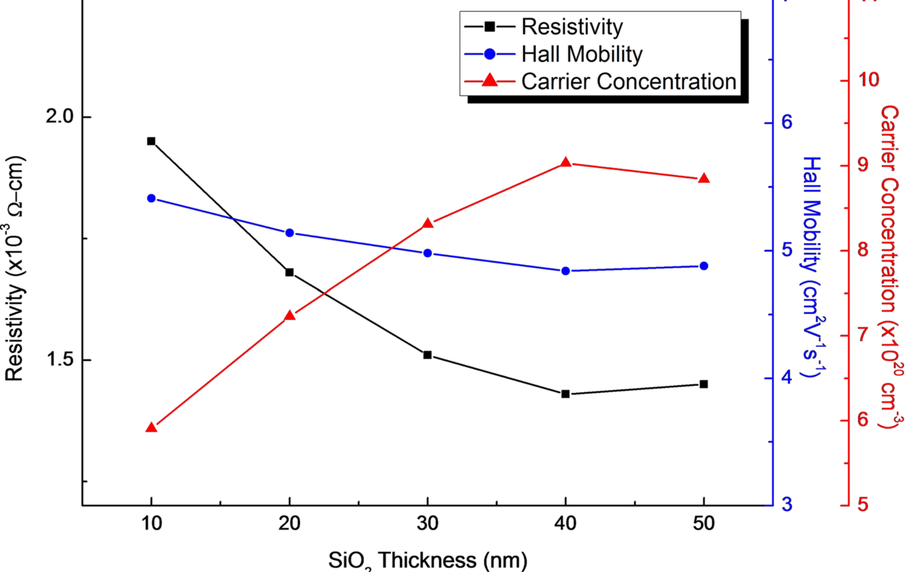

Fig. 9 Resistivity, hall mobility, and carrier concentration of IZTO films deposited on PET with various thicknesses of SiO_2 buffer layers

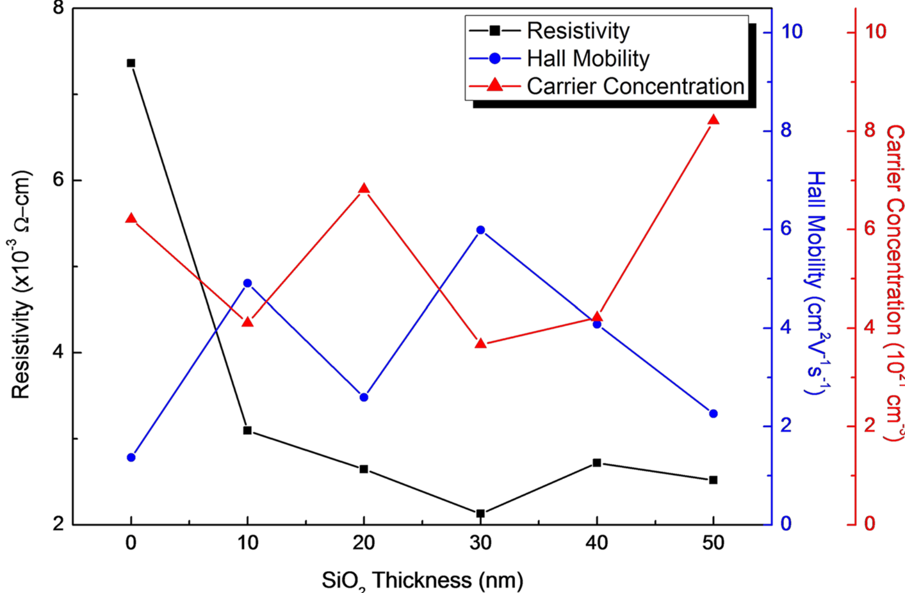

Fig. 10 Resistivity, hall mobility, and carrier concentration of IZTO films deposited on PEN with various thicknesses of SiO_2 buffer layers

layer; this value then decreased as the buffer layer thickness increased. The figure of merit, as shown in Fig. 11, reached its highest value of $6.20\times10^{-4}/\Omega$ when using a 20 nm thick buffer layer, because the figure of merit is more affected by transmittance than sheet resistance, as shown in Eq. (2).

In the case of IZTO thin films deposited on PEN (Fig. 12), the highest sheet resistance value was measured to be 30.667 Ω sq^{-1}, when the buffer layer was not applied. After forming different buffer layer thicknesses ranging from 10 to 50 nm, the IZTO thin films presented superior sheet resistance values of 8.875–12.904 Ω sq^{-1}, compared with the cases in which PET substrates were used. In particular, when using a 30 nm thick buffer layer, the IZTO thin film had the lowest sheet resistance, 8.875 Ω sq^{-1}. As shown in Fig. 8, when no buffer layer was used, PEN substrates yielded a higher transmittance at 550 nm, with a value of 77.19%, compared with the case in which a PET substrate was used. Forming SiO_2 buffer layers with thicknesses ranging from 10 to 50 nm, transmittances at 550 nm were measured to be 70.84, 81.14, 80.26, 74.13, and 71.48%, respectively. When using 20 and 30 nm thick buffer layers on PEN substrates, an excellent transmittance value, higher than 80%, was obtained. By substituting these transmittance and sheet resistance values into Eq. (2), the figure of merit were calculated. Even when not forming a SiO_2 buffer layer, a good figure of merit of $2.45\times10^{-3}/\Omega$

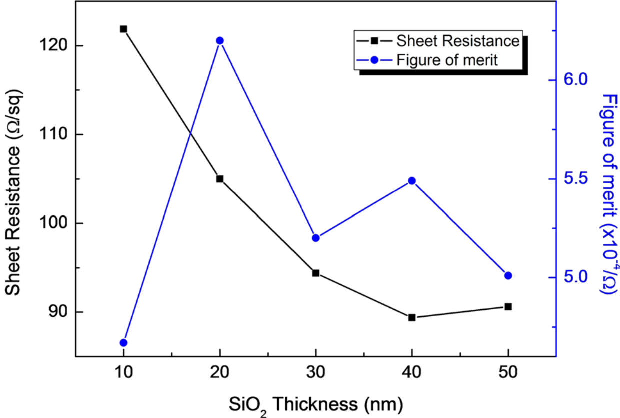

Fig. 11 Sheet resistance and figure of merit for IZTO films deposited on PET with various thickness of SiO_2 buffer layers

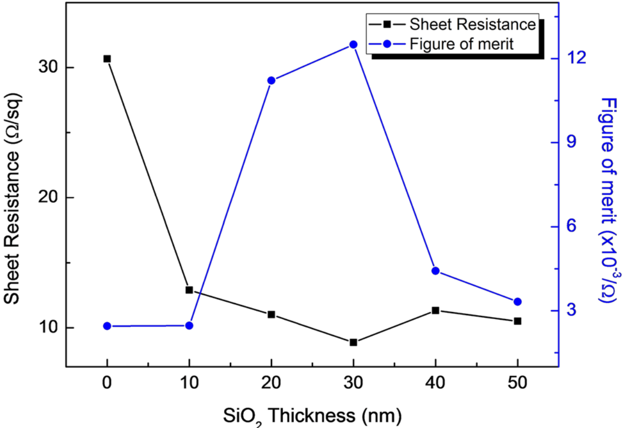

Fig. 12 Sheet resistance and figure of merit for IZTO films deposited on PEN with various thickness of SiO_2 buffer layers

was obtained, which is better than for all the cases in which PET was applied. By forming a buffer layer on PEN, higher figures of merit ranging from 2.46 to $12.50\times10^{-3}/\Omega$ were obtained. In particular, the highest figure of merit was acquired when a 30 nm thick SiO_2 buffer layer was applied.

4 Conclusion

As an effort to develop flexible display devices, IZTO thin films were deposited on plastic substrates (PES, PET, and PEN) using RF magnetron sputtering. The incorrigible problem of plastic substrates, which absorb moisture and gases and then permeate that to the depositing film as impurities, could be alleviated to some degree, by forming a SiO_2 buffer layer before depositing the IZTO thin

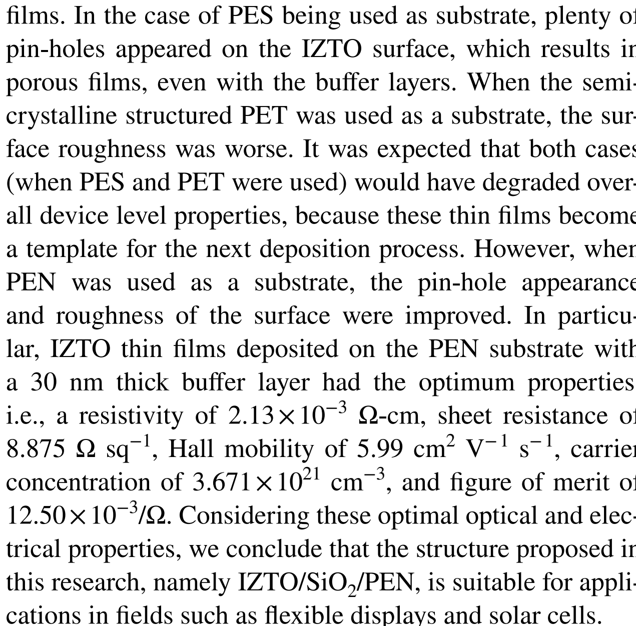
films. In the case of PES being used as substrate, plenty of pin-holes appeared on the IZTO surface, which results in porous films, even with the buffer layers. When the semi-crystalline structured PET was used as a substrate, the surface roughness was worse. It was expected that both cases (when PES and PET were used) would have degraded overall device level properties, because these thin films become a template for the next deposition process. However, when PEN was used as a substrate, the pin-hole appearance and roughness of the surface were improved. In particular, IZTO thin films deposited on the PEN substrate with a 30 nm thick buffer layer had the optimum properties, i.e., a resistivity of 2.13×10^{-3} Ω-cm, sheet resistance of 8.875 Ω sq^{-1}, Hall mobility of 5.99 $cm^2\ V^{-1}\ s^{-1}$, carrier concentration of $3.671\times10^{21}\ cm^{-3}$, and figure of merit of $12.50\times10^{-3}/\Omega$. Considering these optimal optical and electrical properties, we conclude that the structure proposed in this research, namely IZTO/SiO_2/PEN, is suitable for applications in fields such as flexible displays and solar cells.

Acknowledgements This work was supported by INHA UNIVERSITY Research Grant.

References

1. J.H. Kim, K.A. Jeon, G.H. Kim, S.Y. Lee, Appl. Surf. Sci. **252**, 4834 (2006)
2. H. Kim, C.M. Gilmore, A. Pique, J.S. Horwitz, H. Mattoussi, H. Murata, Z.H. Kafafi, D.B. Chrisey, J. Appl. Phys. **86**, 6451 (1999)
3. H. Kim, J.S. Horwitz, G.P. Kushto, Z.H. Kafafi, D.B. Chrisey, Appl. Phys. Lett. **79**, 284 (2001)
4. T. Li, S. Hsu, Eur. Polym. J. **32**, 3368 (2007)
5. V. Teiceira, H. Cui, L. Meng, E. Fortunato, R. Martins, Thin Solid Films **420**, 70 (2002)
6. B. Yaglioglu, Y. Huang, H. Yeom, D. Paine, Thin Solid Films **496**, 89 (2006)
7. Y. Ko, Y. Kim, Mater. Res. Bull. **47**, 2800 (2012)
8. J. Park, S. Kang, Y. Yoon, J. Korean Ceram. Soc. **52**, 224 (2015)
9. Y.Y. Zhang, J. Hu, B.A. Bernevig, X.R. Wang, X.C. Xie, W.M. Liu, Phys. Rev. **102**, 106401 (2009)
10. H. Zhuang, J. Yan, C. Xu, D. Meng, Appl. Surf. Sci. **307**, 241 (2014)
11. X. Ding, J. Yan, T. Li, L. Zhang, Vacuum **86**, 443 (2011)
12. J.H. Chang, S.Y. Liu, I.W. Wu, T.C. Chen, C.W. Liu, C.I. Wu, J. Appl. Phys. **115**, 124510 (2014)
13. J. Park, S. Kang, D. Chang, Y. Yoon, J. Korean Ceram. Soc. **52**, 72 (2015)
14. P. Yang, Y. Ohki, F. Tian, in *ISEIM* (2014), p 401
15. S.H. Kwon, Y.M. Kang, Y.R. Cho, S.H. Kim, P.K. Song, Surf. Coat. Technol. **205**, S312 (2010)
16. P.B. He, X.C. Xie, W.M. Liu, Phys. Rev. B **72**, 172411 (2005)
17. X.L. Zhang, L.F. Liu, W.M. Liu, Sci. Rep. **3**, 2908 (2013)
18. G. Haacke, Ann. Rev. Mater. Sci. **7**, 73 (1977)